A new perspective on warming of the global oceans

M. D. Palmer,[1] S. A. Good,[1] K. Haines,[2] N. A. Rayner,[1] and P. A. Stott[1]

Received 5 June 2009; revised 17 August 2009; accepted 31 August 2009; published 29 October 2009.

[1] Changes in ocean circulation associated with internal climate variability have a major influence on upper ocean temperatures, particularly in regions such as the North Atlantic, which are relatively well-observed and therefore over-represented in the observational record. As a result, global estimates of upper ocean heat content can give misleading estimates of the roles of natural and anthropogenic factors in causing oceanic warming. We present a method to quantify ocean warming that filters out the natural internal variability from both observations and climate simulations and better isolates externally forced air-sea heat flux changes. We obtain a much clearer picture of the drivers of oceanic temperature changes, being able to detect the effects of both anthropogenic and volcanic influences simultaneously in the observed record. Our results show that climate models are capable of capturing in remarkable detail the externally forced component of ocean temperature evolution over the last five decades. **Citation:** Palmer, M. D., S. A. Good, K. Haines, N. A. Rayner, and P. A. Stott (2009), A new perspective on warming of the global oceans, *Geophys. Res. Lett.*, *36*, L20709, doi:10.1029/2009GL039491.

1. Introduction

[2] Increases in greenhouse gas concentrations have caused excess heat to build up in the climate system and it has been estimated that over 80% of this heat has accumulated in the global oceans [*Levitus et al.*, 2005]. Therefore, the observed rate of ocean warming provides one of the best indicators of the global radiation imbalance. The uptake of heat by the ocean acts to mitigate transient surface temperature rise. It is essential to carefully evaluate this process in climate models in order to have appropriate confidence in their predictions.

[3] One of the challenges for climate model evaluation is that observational data sets have a strong imprint of natural variability associated with climate modes, such as ENSO (El Niño – Southern Oscillation). This can be particularly problematic for sparsely sampled data, such as historical observations of the subsurface ocean. Therefore, careful model-observation comparisons should be carried out based upon understanding of the underlying processes that have shaped the observational record.

[4] The average temperature of the water column at a particular location can be changed in one of two ways. First, changes in air-sea heat flux can cause the column average temperature to go up or down. Second, the column average temperature can be changed by advective redistribution of oceanic heat. In the present study, we are most interested in air-sea heat flux changes. This is the primary direct mechanism by which we expect the oceans to respond to anthropogenic greenhouse gas warming and other natural climate forcings, such as volcanic aerosols.

[5] The difficulty with analyses of ocean warming using the conventional "fixed depth" approach, e.g., the IPCC AR4 [*Bindoff et al.*, 2007], is that these two mechanisms cannot be separated. It was recently estimated that approximately 50% of the upper ocean warming signal in the North Atlantic could be associated purely with changes in ocean circulation [*Palmer and Haines*, 2009]. The North Atlantic and North Pacific are certainly over-represented compared to other basins, with consistently the best observational coverage throughout the historical record. Such sampling problems can easily confound basin or global average warming rates unless great care is taken [e.g., *Gregory et al.*, 2004].

[6] When evaluating the signals of ocean warming in climate models, it is normal practice to use an ensemble of model simulations. While a single model simulation could, in principle, reproduce advective signals associated with changes in the large-scale climate modes, these signals are unlikely to have the same phase as those observed in the real climate system. Climate mode changes represent the unforced, internal variability of the system, which is reduced in model simulations by averaging over the model ensemble. Therefore we are always likely to see some mismatch between models and observations originating from the internal variability that remains in the observed record. Here we show that if we can better isolate signals associated with changes in air-sea heat fluxes (rather than advection) in both the data and the models we see a dramatic improvement in the comparison between model simulations and the observations.

2. Data and Methods

[7] We present a model-data comparison using two different indicators of ocean warming: (i) the average temperature over the upper 220 m (T_{220m}), similar to methods used in the IPCC AR4; and (ii) the average temperature above the 14°C isotherm (T_{14C}), following the approach of previous studies [*Palmer et al.*, 2007; *Palmer and Haines*, 2009]. We choose the 14°C isotherm because it provides good coverage of the upper water column, at low to mid-latitudes, throughout the historical record, and 220 m because it is the overall time-spatial mean depth of the 14°C isotherm. As noted in earlier investigations [*Stevenson and Niiler*, 1983; *Toole et al.*, 2004], T_{14C} should provide a better indication of changes in air-sea heat fluxes, through removal of dynamically-driven vertical advection in the heat

[1]Met Office Hadley Centre, Exeter, UK.
[2]Environmental Systems Science Centre, University of Reading, Reading, UK.

0094-8276/09/2009GL039491$05.00

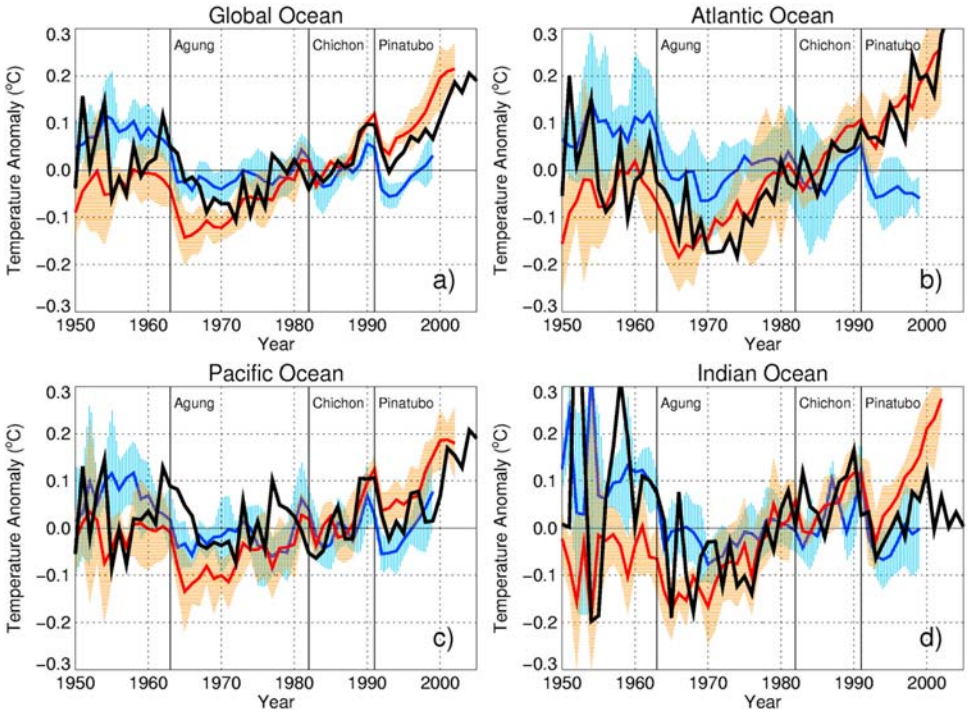

Figure 1. Time series of global ocean temperature above 220 m (T_{220m}) relative to 1950–1999 average, for (a) Global Ocean, (b) Atlantic Ocean (c) Pacific Ocean, and (d) Indian Ocean. Shown are: the XBT-corrected observations (black); the HadCM3 ALL ensemble average (red) and ensemble standard deviation (orange shading); and the HadCM3 NAT ensemble average (blue) and ensemble standard deviation (light blue shading). The model data have been re-gridded and sub-sampled to match the observational coverage. The vertical lines show the approximate timing of the major volcanic eruptions.

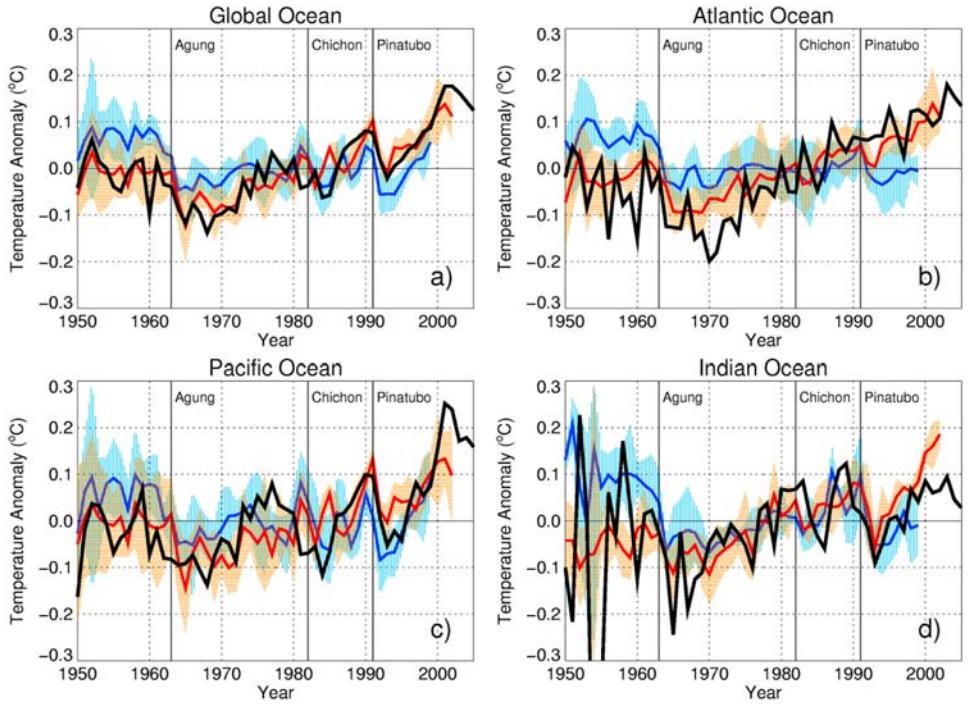

Figure 2. As for Figure 1, but for temperature above the 14°C isotherm (T_{14C}) relative to 1950–1999 average, for (a) Global Ocean, (b) Atlantic Ocean (c) Pacific Ocean, and (d) Indian Ocean. Shown are: the XBT-corrected observations (black); the HadCM3 ALL ensemble average (red) and ensemble standard deviation (orange shading); and the HadCM3 NAT ensemble average (blue) and ensemble standard deviation (light blue shading). The model data have been re-gridded and sub-sampled to match the observational coverage. The vertical lines show the approximate timing of the major volcanic eruptions.

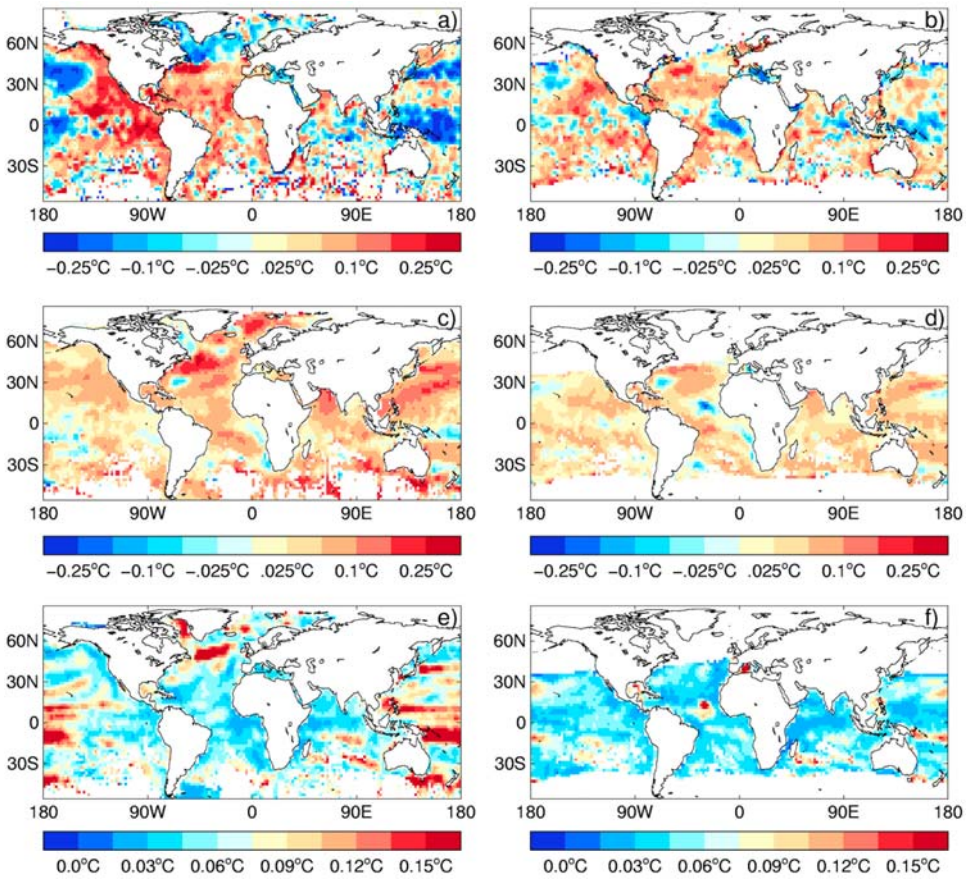

Figure 3. Spatial maps of temperature trends (°C per decade) computed from the EN3 observations for (a) average temperature above 220 m (T_{220m}), and (b) average temperature above 14°C (T_{14C}). (c and d) Equivalent maps for the HadCM3 climate model "All Forcings" ensemble average. (e and f) Standard deviation of the HadCM3 ensemble trends for T_{220m} and T_{14C}, respectively. The model data have been re-gridded and sub-sampled to match the observational coverage. Each plot has had a 1:2:1 grid-scale smoothing applied in the North-South and East-West direction to reduce the sampling noise.

budget. The main limitation of the isotherm approach, compared to conventional methods, is that it cannot be easily applied at the high latitudes, where temperature inversions are problematic.

[8] The observations used are the Met Office Hadley Centre EN3 quality-controlled temperature profiles [*Ingleby and Huddleston*, 2007] (available from www.metoffice.gov.uk/hadobs), which span the period 1950-present. We apply the XBT bias-corrections [*Wijffels et al.*, 2008] used in a recent re-evaluation of the steric contribution to global sea-level rise [*Domingues et al.*, 2008], but note that T_{14C} measurements are insensitive to these corrections [*Palmer et al.*, 2007]. T_{14C} and T_{220m} are computed for each profile separately and values for each month are averaged into 2° × 2° latitude-longitude grid boxes [*Palmer et al.*, 2007].

[9] The climate simulations come from the Met Office Hadley Centre HadCM3 coupled climate model [*Gordon et al.*, 2000]. We use four-member ensemble simulations of the 20th century under: (i) anthropogenic (ANT) external forcings; (ii) natural (NAT) external forcings; and (iii) combined anthropogenic and natural forcings (ALL). ANT includes the effects of greenhouse gases and anthropogenic aerosols, NAT includes only solar and volcanic aerosol forcings, and ALL uses the combined ANT and NAT forcings [*Stott et al.*, 2000]. We sub-sample the model at the same location as the observations to avoid introducing uncertainty associated with in-filling of the observations [*Gregory et al.*, 2004].

[10] The optimal detection results presented here are based on a five-point spatial model fingerprint, composed of the average temperature anomaly in the North Atlantic, South Atlantic, North Pacific, South Pacific and Indian Oceans, relative to the period 1950–1999. Annual-average model data were re-gridded and sub-sampled to match the observational coverage. Annual averages were produced for the observed data by combining the gridded monthly fields in each year, after removing the seasonal cycle. All data were averaged into 2-year bins to reduce the observational sampling noise, resulting in twenty-five time slices of the five-point fingerprint. Please see the auxiliary material for further information.[1]

3. Results

[11] The ALL simulations, which include anthropogenic forcings, show considerably better agreement with the

[1] Auxiliary materials are available in the HTML. doi:10.1029/2009GL039491.

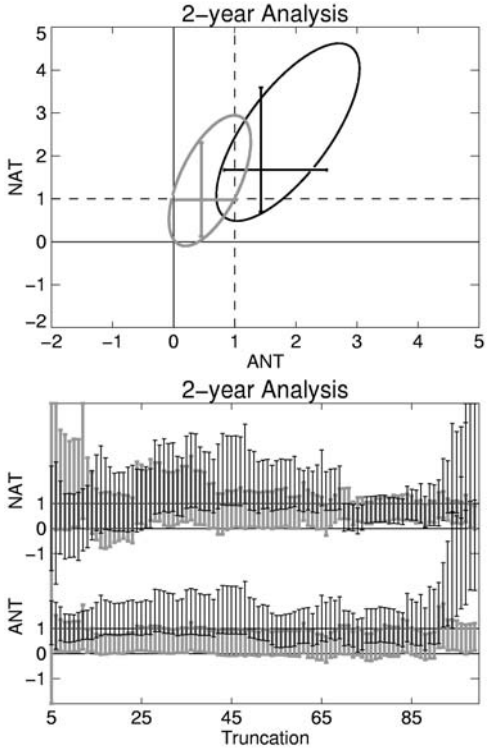

Figure 4. (a) the estimated scaling factors of ANT and NAT projected onto the observations, using a truncation value of 30. The 95% confidence interval is represented by the ellipses and error bars. (b) The scaling factors with 95% confidence intervals for EOF all truncation values. The T_{14C} results are shown in black and the T_{220m} results are shown in grey. The external forcing is said to be ''detected'' in the observations if the corresponding scaling factor is significantly non-zero. If, in addition, the scaling factor is consistent with unity, the simulated model response is consistent with the observations. A scaling factor smaller than unity indicates that the response is over estimated in the model simulation, and vice versa.

observations than the NAT simulations (Figures 1 and 2). As well as the long-term rise in ocean temperature for the ALL ensemble, we can see the short-lived cooling events associated with major volcanic eruptions in 1963, 1982 and 1991 in both the ALL and NAT simulations. The 1982 event is not so clear in the observations, since it was coincident with a large El Niño, which offset the volcanic cooling. The divergence of the observed and simulated time series for the Indian Ocean after 1992 (Figures 1 and 2) may be related to regional cooling by anthropogenic aerosols that are not represented in the HadCM3 forcings [*Ramanathan et al.*, 2005]. The T_{14C} results show a 15–40% reduction in the RMS error between model ensemble-mean and the observations compared to the T_{220m} analysis, depending on ocean basin (Table S1). This result is consistent with the idea that we have successfully reduced the influence of ocean circulation changes in the observations for the T_{14C} analysis.

[12] A more spatially uniform pattern of warming is seen for T_{14C} than for T_{220m} in the observations (Figures 3a and 3b), in agreement with previous studies [*Palmer et al.*, 2007]. Changes in T_{220m} are highly correlated with changes in the depth of the 14°C isotherm (not shown). Comparing the same maps from the model ensemble means, the T_{14C} map shows qualitatively better agreement between model and observations than the T_{220m} map (Figures 3c and 3d). We suggest that this is because ocean circulation changes play a large role in the observed T_{220m} trend maps, but these are largely averaged out in the model ensemble mean. The reduction of ocean circulation influences, associated with internal variability, on T_{14C} is further supported by the reduced variance in the spatial trends compared to T_{220m} (Figures 3e and 3f).

4. Optimal Detection Analysis

[13] Finally, we carry out an optimal detection analysis [*IDAG*, 2005] on T_{14C} and T_{220m} to attribute the observed ocean warming to anthropogenic and/or natural causes. The optimal detection analysis determines whether the expected anthropogenic and natural ''fingerprints'' have emerged significantly in the observations, above the ''noise'' of internal variability. Previous studies have detected only the secular anthropogenic warming influences on the oceans [*Barnett et al.*, 2001, 2005; *Pierce et al.*, 2006]. Here we use a finer temporal resolution that allows us to also investigate the response to natural external forcings (volcanoes, solar). The optimal detection analysis compares the observed and model simulated spatio-temporal patterns of ocean warming (see section 2). A necessary requirement for an optimal detection analysis is that the model adequately simulates the observed internal variability. This requirement is met for both T_{14C} and T_{220m}, as shown in Figure S1.

[14] The truncation values referred to in Figure 4 correspond to the number of empirical orthogonal functions (EOFs) used in the optimal detection analysis. Detection of an anthropogenic or natural influence is robust if it is insensitive to the number of EOFs used (over a wide range of truncation values). See the auxiliary material for further details. Both anthropogenic and natural forcings are robustly detected using T_{14C} and the magnitude of the response in the HadCM3 model is consistent with the observations (Figure 4). In contrast, we do not find a robust detection of either signal for T_{220m} and the model appears to over estimate the observed response to anthropogenic forcings. The robust detection for T_{14C} may be due in part to the reduced observational sampling noise associated with filtering of high frequency ocean dynamics [*Palmer et al.*, 2007] (e.g., eddies, internal waves).

5. Conclusions

[15] The historical climate records contain a strong imprint of internal variability associated with the state of climate mode evolution at the time the observations were taken. We have reduced the internal variability in the observations by computing ocean temperature changes relative to a fixed isotherm, rather than a fixed depth, which better isolates the externally forced air-sea heat flux signals. Climate mode variability is similarly reduced in the climate model simulations, resulting in a much improved observation-model comparison and a robust detection of both natural and anthropogenic influences on ocean subsurface temperatures

for the first time. The detection results presented in this paper would be strengthened by the use of a larger, multi-model ensemble. Nevertheless, in demonstrating such a level of agreement between observations and climate simulations, our isotherm technique paves the way for observationally-constrained estimates of future increases in ocean heat content and sea level rise.

[16] **Acknowledgments.** MDP, SAG, NAR and PAS were supported by the Joint DECC/Defra (GA01101) and MoD (CBC/2B/0417_Annex C5) Integrated Climate Programme. KH was supported by the Natural Environment Research Council under the NCEO program and by sponsorship from the BMT group. We thank Gareth Jones for useful discussions and an anonymous reviewer for their contributions to improving this paper.

References

Barnett, T. P., D. W. Pierce, and R. Schnur (2001), Detection of anthropogenic climate change in the world's oceans, *Science*, *292*, 270–274, doi:10.1126/science.1058304.

Barnett, T. P., D. W. Pierce, K. M. AchutaRao, P. J. Glecker, B. D. Santer, J. M. Gregory, and W. M. Washington (2005), Penetration of human-induced warming into the world's oceans, *Science*, *309*, 284–287, doi:10.1126/science.1112418.

Bindoff, N. L., et al. (2007), Observations: Oceanic climate change and sea level, in *Climate Change 2007: The Physical Science Basis. Contribution of Working Group I to the Fourth Assessment Report of the Intergovernmental Panel on Climate Change*, edited by S. Solomon et al., chap. 5, pp. 385–432, Cambridge Univ. Press, Cambridge, U. K.

Domingues, C. M., J. A. Church, N. J. White, P. J. Gleckler, S. E. Wijffels, P. M. Barker, and J. R. Dunn (2008), Improved estimates of upper-ocean warming and multi-decadal sea-level rise, *Nature*, *453*, 1090–1094, doi:10.1038/nature07080.

Gordon, C., C. Cooper, C. A. Senior, H. Banks, J. M. Gregory, T. C. Johns, J. F. B. Mitchell, and R. A. Wood (2000), The simulation of SST, sea ice extents and ocean heat transports in a version of the Hadley Centre coupled model without flux adjustments, *Clim. Dyn.*, *16*, 147–168, doi:10.1007/s003820050010.

Gregory, J. M., H. T. Banks, P. A. Stott, J. A. Lowe, and M. D. Palmer (2004), Simulated and observed decadal variability in ocean heat content, *Geophys. Res. Lett.*, *31*, L15312, doi:10.1029/2004GL020258.

Ingleby, B., and M. Huddleston (2007), Quality control of ocean temperature and salinity profiles—Historical and real time data, *J. Mar. Syst.*, *65*, 158–175, doi:10.1016/j.jmarsys.2005.11.019.

International Ad Hoc Detection and Attribution Group (IDAG) (2005), Detecting and attributing external influences on the climate system: A review of recent advances, *J. Clim.*, *18*, 1291–1314, doi:10.1175/JCLI3329.1.

Levitus, S., J. I. Antonov, and T. P. Boyer (2005), Warming of the world ocean, 1955–2003, *Geophys. Res. Lett.*, *32*, L02604, doi:10.1029/2004GL021592.

Palmer, M. D., and K. Haines (2009), Estimating oceanic heat content change using isotherms, *J. Clim.*, in press.

Palmer, M. D., K. Haines, S. F. B. Tett, and T. J. Ansell (2007), Isolating the signal of ocean global warming, *Geophys. Res. Lett.*, *34*, L23610, doi:10.1029/2007GL031712.

Pierce, D. W., T. P. Barnett, K. AchutaRao, P. J. Glecker, J. M. Gregory, and W. M. Washington (2006), Anthropogenic warming of the oceans: Observations and model results, *J. Clim.*, *19*, 1873–1900, doi:10.1175/JCLI3723.1.

Ramanathan, V., C. Chung, D. Kim, T. Bettge, L. Buja, J. T. Kiehl, W. M. Washington, Q. Fu, D. R. Sikka, and M. Wild (2005), Atmospheric brown clouds: Impacts on South Asian climate and hydrological cycle, *Proc. Natl. Acad. Sci. U. S. A.*, *102*, 5326–5333, doi:10.1073/pnas.0500656102.

Stevenson, J. W., and P. P. Niiler (1983), Upper ocean heat budget during the Hawaii-to-Tahiti shuttle experiment, *J. Phys. Oceanogr.*, *13*, 1894–1907, doi:10.1175/1520-0485(1983)013<1894:UOHBDT>2.0.CO;2.

Stott, P. A., S. F. B. Tett, G. S. Jones, M. R. Allen, J. F. B. Mitchell, and G. J. Jenkins (2000), External control of twentieth century temperature by natural and anthropogenic causes, *Science*, *290*, 2133–2137, doi:10.1126/science.290.5499.2133.

Toole, J. M., H.-M. Zhang, and M. J. Caruso (2004), Time-dependent internal energy budgets of the tropical warm water pools, *J. Clim.*, *17*, 1398–1410, doi:10.1175/1520-0442(2004)017<1398:TIEBOT>2.0.CO;2.

Wijffels, S. E., J. Willis, C. M. Domingues, P. Baker, N. J. White, A. Gronell, K. Ridgway, and J. A. Church (2008), Changing expendable bathythermograph fall-rates and their impact on estimates of thermosteric sea level rise, *J. Clim.*, *21*, 5657–5672, doi:10.1175/2008JCLI2290.1.

S. A. Good, M. D. Palmer, N. A. Rayner, and P. A. Stott, Met Office Hadley Centre, FitzRoy Road, Exeter EX1 3PB, UK. (matthew.palmer@metoffic.gov.uk)

K. Haines, Environmental Systems Science Centre, University of Reading, Harry Pitt Building, P.O. Box 238, Reading RG6 6AL, UK.